Abstract

Resolution of Chronic Granulomatous Inflammation and Fibrosis in a Murine Model of Sarcoidosis

by

Sophia J. Bhalla

July 2021

Director of Thesis: Mary Jane Thomassen, PhD, Department of Internal Medicine

MS Program in Biomedical Sciences

Sarcoidosis is a chronic granulomatous disease of unknown cause. Granulomas resolve within 12-26 months in 50% of cases without therapy while 30% of patients have chronic disease that progresses to pulmonary fibrosis. The transcription factor peroxisome proliferator activated receptor gamma (PPARγ), a negative regulator of pro-inflammatory macrophage activation, is deficient in the alveolar macrophages of sarcoidosis patients. We established a chronic murine model of sarcoidosis in which multiwall carbon nanotubes (MWCNTs) are administered via oropharyngeal instillation. The expression of PPARγ is also deficient in the murine alveolar macrophages. Granulomatous lesions persist for at least 90-days post installation. Previous studies from our lab have implicated matrix metalloproteinase-12 (MMP12) and osteopontin (OPN) as key factors that work together to promote granuloma formation and persistence. We used a macrophage-specific PPARγ knockout mouse to study the effects of PPARγ deficiency on sarcoidosis pathophysiology. As expected, PPARγ mice had more robust granuloma formation at 60-days post instillation compared to C57BL/6J controls. We hypothesized that PPARγ mice

would have large, persisting granulomatous structures 90-days post instillation and that levels of MMP12 and OPN would be elevated. PPARγ and C57BL/6J mice were instilled with MWCNT. Controls received PBS alone. Lung tissue from both strains were sectioned, stained, and subjected to granuloma scoring and qualitative evaluation. Tissue from PPARγ mice was also used for immunohistochemistry (IHC). Surprisingly, at 90-days post instillation, PPARγ mice had attenuated fibrosis and decreased granuloma size compared to 60-days and C57BL/6J mice. Evaluation of mediators in the canonical TGFβ signaling pathway did not explain the changes in fibrosis. Changes in MMP12 and OPN protein levels, however, were apparent. Immunohistochemistry of lung tissue showed decreased expression of both MMP12 and OPN at 90-days post instillation. These results suggest a relationship between MMP12 and OPN in the resolution of granulomatous structures. The decrease in MMP12 and OPN in tissue sections at 90-days is especially important as pulmonary granulomatous structures form and resolve within lung tissue.

Resolution of Chronic Granulomatous Inflammation and Fibrosis in a Murine Model of Sarcoidosis

A Thesis Presented to

The Faculty of the MS Program in Biomedical Sciences

Office of Research and Graduate Studies at Brody School of Medicine

In Association with the Department of Internal Medicine, Brody School of Medicine

Submitted in Partial Fulfillment

of the Requirements for the Degree

Master's of Science

Biomedical Sciences

by

Sophia J. Bhalla

July 2021

Resolution of Chronic Granulomatous Inflammation and Fibrosis in a Murine Model of Sarcoidosis

by

Sophia J. Bhalla

APPROVED BY:

DIRECTOR OF THESIS: _____

Mary Jane Thomassen, Ph.D.

COMMITTEE MEMBER: _____

Arjun Mohan, M.D.

COMMITTEE MEMBER: _____

Ogugua Obi, M.D.

COMMITTEE MEMBER: _____

Rukiyah Van Dross, Ph.D.

DIRECTOR, MS PROGRAM
IN BIOMEDICAL SCIENCES: _____

Richard Franklin, Ph.D.

DEAN OF THE
GRADUATE SCHOOL: _____

Paul Gemperline, Ph.D.

ACKNOWLEDGEMENTS

This work was supported by the National Institutes of Health (NIH) grant ES025191 (MJ Thomassen).

TABLE OF CONTENTS

LIST OF TABLES

CHAPTER 4

LIST OF FIGURES

CHAPTER 1

CHAPTER 3

CHAPTER 4

LIST OF ABBREVIATIONS

2°: secondary

AM: alveolar macrophages

ANOVA: analysis of variance

BAL: bronchoalveolar lavage

C: celcius

c-Abi: c-application binary interface

CCL2: C-C motif chemokine ligand 2

CCL20: C-C motif chemokine ligand 20

cDNA: complementary deoxyribonucleic acid

CT: cycle threshold

CTSK: cathepsin K

ELISA: enzyme-linked immunosorbent assay

Erk1/2: extracellular signal-regulated kinase 1/2

FDNY: Fire Department of the City of New York

GAPDH: glyceraldehyde 3-phosphate dehydrogenase

HLA: human leukocyte antigen

H&E: hematoxylin and eosin

IFNγ: interferon gamma

IL-1: interleukin 1

IL-12: interleukin 12

IL-17: interleukin 17

LCK: lymphocyte-specific protein tyrosine kinase

LSM: laser scanning microscope

Lym: lymphocytes

MHC: major histocompatibility complex

ml: milliliter

MMP12: matrix metallopeptidase 12

mRNA: messenger RNA

MWCNT: multi-wall carbon nanotubes

OCT: optimal cutting temperature

OPN: osteopontin

PPARγ: peroxisome proliferator-activated receptor gamma

PBS: phosphate buffered solution

PMN: polymorphonuclear cells

qPCR: quantitative polymerase chain reaction

rpm: rotations per minute

SEM: standard error of the mean

SD: standard deviation

SMAD3: mothers against decapentaplegic homolog 3

SMAD7: mothers against decapentaplegic homolog 7

STAT4: signal transducer and activator of transcription 4

TBE: tribromoethanol

TGFβ: transforming growth factor beta

TNFα: tumor necrosis factor alpha

µg: microgram

µL: microliter

Δ: change in

°: degrees

CHAPTER 1:

Introduction

1.1 Sarcoidosis

Sarcoidosis is a multisystemic disease characterized by noncaseating granulomatous inflammation that is found predominantly in the lungs and lymph nodes. Rates of disease vary by race, ethnicity, and geographical location. Prevalence is highest in Nordic countries and in African American individuals at 160 and 141.4 per 100,000 respectively (1, 2). Caucasians, Hispanics, and Asians in the United States have lower disease prevalence at 49.8, 21.7, and 18.9 per 100,000 (2). Sarcoidosis affects women more often than men and in America, African American women have the highest disease prevalence at 178.5 per 100,000 (2, 3). The peak age of onset currently ranges between 30 and 55 years of age (4). This age range has increased over time, a trend that could be due to an aging population, changes in detection, and shifts in exposure to environmental factors.

Sarcoidosis is a difficult disease to diagnose. The disease can affect every organ in the body and severity ranges from asymptomatic cases to life-threatening disease states. The lungs are the most involved organ, affecting 90% of patients (5). The skin, eyes, liver, and peripheral lymph nodes are implicated in 10-30% of cases (5). There is no specific test for detection of sarcoidosis, however, experts have developed criteria that must be met prior to assigning a diagnosis: clinical or radiological findings consistent with the condition and a tissue biopsy with evidence of noncaseating granulomas (3).

Pulmonary sarcoidosis has varying presentations. The most common symptoms are dyspnea and cough. The latter is reported in 90% of patients. Wheezing, chest pain, and fatigue are other frequent manifestations. Chest radiographs are abnormal in 90% of cases. Radiographic abnormalities can uncover disease in asymptomatic individuals, which account for 50% of patients, whereas respiratory failure is a hallmark of progressive pulmonary cases (6).

Bilateral hilar adenopathy and parenchymal lung opacities affect 50-85% and 25-60% of patients respectively. Pulmonary fibrosis is evident in up to 30% of cases and can cause respiratory failure, pulmonary hypertension, and hemoptysis which can lead to permanent organ damage and death (3, 5). Fibrosis is present in the majority of deaths from pulmonary sarcoidosis (5).

To account for the diversity of disease presentation, The Siltzbach Classification System was developed to define five stages of sarcoidosis based on chest radiographic findings. Cases are assigned accordingly: stage 0 is classified by a normal chest radiograph; stage 1 indicates lymphadenopathy only; stage 2 is marked by lymphadenopathy and parenchymal lung disease; stage 3 is defined by parenchymal lung disease only; and stage 4 signifies fibrosis (6). Conditions can regress, remain stable, or progress through the stages. Progression to pulmonary fibrosis occurs in 30% of patients (6).

Granulomas resolve within 12-36 months in 50% of cases without therapy (7). Therefore, current best practices indicate that treatment should only be initiated in the presence of granulomatous inflammation, pulmonary dysfunction, and symptoms that affect quality of life (8). Symptoms hold the most weight when considering treatment. Corticosteroids are the drug of choice; however, they are associated with significant side effects and are used sparingly (8).

1.2 Sarcoidosis etiology

Sarcoidosis is a granulomatous disease of unknown cause. The condition is viewed as a consequence of a chronic immunological response and has been associated with genetic susceptibilities and environmental factors. Clusters of cases within families and increased prevalence among certain ethnic and racial groups supports a genetic component to the disease

(7, 9, 10). Genetic predispositions that have been linked to an increased risk of sarcoidosis have most frequently been associated with the major histocompatibility complex (MHC) region on chromosome 6, also known as the human leukocyte antigen (HLA) system (9, 11). The primary biological role of this genetic loci is the regulation of immune responses. HLA genes are known to be involved in the rejection of foreign bodies, in antigen presentation, and in regulating adaptive immunity (9, 11). Derived molecules are divided into two classes; class I molecules are expressed on the surface of most nucleated cells whereas class II molecules are only expressed on the surfaces of B lymphocytes, antigen-presenting cells (monocytes, macrophages, and dendritic cells), and activated T lymphocytes (11). Certain polymorphisms of class I and class II HLA alleles have been associated with increased risk of sarcoidosis development (7, 9, 11). Stronger associations have been observed for class II molecules (7, 9).

Sarcoidosis is a complex disease. In addition to genetic factors, multiple infectious agents have been identified as possible triggers. Studies have suggested an etiological link between mycobacteria and the disease; however, the data is inconsistent. Some studies have identified mycobacterial components in sarcoid tissue while others have not (12). *Propionibacterium acnes* have also been implicated as the skin bacterium has been cultured from sarcoidosis granulomas (12). Additional infectious agents linked to the disease include fungi and borrelia. Sarcoidosis is also associated with environmental exposures including non-infectious organic antigens, metals, combustible products, and inorganic substances. Epidemiological studies have shown an association between certain environments and sarcoidosis prevalence. At risk populations include those who have high exposure to microbes (i.e. agricultural settings and exposure to certain water sources), inorganic dusts (i.e. mining and construction), and byproducts of combustion (i.e. firefighters and first responders) (7, 9, 12).

Research has shown that firefighters experience a higher incidence of sarcoidosis compared to the general population. Between 1985 and 1998, firefighters from the Fire Department of the City of New York (FDNY) had an annual incidence of disease of 12.9 per 100,000, a rate several folds higher than other service workers (13, 14). This trend was exacerbated after the World Trade Center attack in 2001. It is estimated that 60-70,000 first responders were exposed to a cloud of toxic dust and smoke generated from the collapse of the towers (13-15). Subsequently, the incidence of sarcoidosis in FDNY firefighters doubled to 25 per 100,000 between 2002 and 2015 (13). This result is currently explained as a consequence of intense exposure to products of combustion of jet fuel, building materials, glass, silica, heavy metals, and organic compounds (15). Case studies have shown carbon nanoparticles in lung biopsy specimens of patients with persistent lung disease after the attack, highlighting a potential disease trigger (15).

Decades of research have not uncovered a single explanation for sarcoidosis presentation. Instead, the diverse genetic and environmental clues indicate that sarcoidosis could either represent a collection of conditions that result in multisystemic granulomatous disease or that the varying exposures each stimulate a specific pathway that promotes sarcoidosis (12).

1.3 Pulmonary Granulomas

Noncaseating granulomas are the histological hallmark of sarcoidosis. The lesions are most commonly found in the lungs and lymph nodes (7). Monocytes and macrophages are the first cells to be recruited to the site of initiation. The cells accumulate and mature into epithelioid cells. T and B lymphocytes, fibroblasts, and other matrix-associated cells infiltrate

the cell aggregates and organize into compact lesions. Finally, T lymphocytes and macrophages release mediators, such as cytokines and chemokines, which amplify the immune response resulting in the recruitment of additional immune cells (7, 9). This process is a pathological response to an offending agent that creates a physical barrier to prevent harm to the surrounding tissue. In 50% of sarcoidosis cases, the granulomas resolve within 12-36 months (7). However, in up to 30% of cases, the lesions persist chronically, causing prolonged inflammation and fibrosis (5). Pulmonary fibrosis can lead to changes in pulmonary function, organ failure, and death. It is important to study the mechanisms of granuloma formation, persistence, and resolution to further understand this disease in hopes of uncovering targets for treatment.

1.4 Multiwall carbon nanotube murine model of sarcoidosis

Several murine models have been created to study sarcoidosis. Microbe-related agents and antigen-bound Sepharose beads have commonly been used to induce granuloma formation (16-18). Resolution of these lesions within 14-21 days has been a leading limitation of studies using these methods. The rapid degradation makes it difficult to distinguish between biological responses to initial injury, granuloma formation, and resolution. Our multiwall carbon nanotube (MWCNT) murine model evades this constraint as granulomas persist for at least 90-days post instillation (19).

Carbon nanotubes are hydrophobic carbon cylinders whose diameter can range from a few nanometers to 200 nanometers in length (15). MWCNTs are concentrically stacked carbon cylinders with a common long axis. The particles can be synthesized commercially or can be developed at high temperatures in the presence of carbon and a metal catalyst (15). As

mentioned previously, these carbon nanotubes have been found in lung biopsy specimens of World Trade Center responders, a population that has experienced an increased incidence of sarcoidosis since the attack (13-15). These findings prompted the development of our murine model in which MWCNTs are administered via oropharyngeal instillation to study pulmonary granulomas.

The MWCNT model bears several similarities to human sarcoidosis patients. Histologically, both experience an aggregation of macrophages which can progress to giant cells during granuloma formation (20). A transcriptional survey revealed that the model shares commonly activated processes with the patient population including T-cell signaling, IL-12 and IL-17 pathways, IFNγ signaling, apoptosis, and oxidative phosphorylation (20). Common upregulated genes involved in immune responses and matrix remodeling have been identified including STAT4, LCK, MMP12, and CTSK (20). As a chronic model of granulomatous disease that bears similarities to human sarcoidosis, the MWCNT model provides a means to study mechanisms of disease progression and resolution.

1.5 Alveolar macrophages contribute to pulmonary inflammation and resolution

Alveolar macrophages are mononuclear phagocytes found in the pulmonary alveoli. As part of the innate immune system, they serve as the first line of defense against respiratory pathogens. As regulators of homeostasis, they communicate with many cell types including epithelial cells, endothelial cells, neutrophils, lymphocytes, fibroblasts, progenitor cells, and other macrophages (21). Macrophage presence is crucial for pathogen recognition, resolution of lung inflammation, and repair of damaged tissue. When faced with an influx of infectious

agents, alveolar macrophages recruit immune cells such as neutrophils to the site of infection and secrete several proinflammatory cytokines and chemokines including interleukins 1, -6, and -8 and tumor necrosis factor (21, 22). After the infectious substance has been addressed, the cells play a role in resolution of inflammation in the airspace. The cells possess remarkable plasticity and can adopt pro-inflammatory, pro-fibrotic, anti-inflammatory, or anti-fibrotic properties based on the lung microenvironment in effort to maintain tissue homeostasis (21, 22).

Alveolar macrophages have been implicated in sarcoidosis granuloma formation. Studies have shown that alveolar macrophages from sarcoidosis patients produce increased amounts of inflammatory cytokines, such as TNFα and IL-1, compared to healthy controls (23). The production of CCL20, a chemokine known to attract dendritic cells and T cells, is also increased (23). Experimentation in murine models has supported these findings (23). Current literature suggests that upon initial injury, alveolar macrophages are triggered causing them to release cytokines and recruit immune cells and additional macrophages, resulting in granuloma formation (19). As versatile cells implicated in a variety of immune responses and tissue homeostasis, alveolar macrophages are likely involved in the degradation of granulomatous structures. Their gene expression and protein are at the center of current studies of granuloma resolution.

1.6 Sarcoidosis patients and MWCNT-instilled mice experience macrophage-specific PPARγ deficiency

Peroxisome proliferator-activated receptor gamma (PPARγ) is a ligand-dependent transcription factor and a member of the nuclear receptor subfamily (24). It is a known regulator

of adipocyte differentiation and glucose homeostasis and has also become recognized as a negative regulator of inflammatory genes (25-27). PPARγ has been shown to antagonize the activities of several transcription factors including AP-1, STAT, and NFκB (25).

PPARγ is constitutively expressed in healthy individuals, however, expression is reduced in patients with pulmonary sarcoidosis, suggesting PPARγ may be a critical factor in limiting pulmonary inflammation (27, 28). These findings have been supported within our murine model. MWCNT instilled C57BL/6J mice exhibit decreased PPARγ mRNA and protein production and DNA binding activity 60-days post instillation (27). These findings suggest that PPARγ is a negative regulator of granuloma formation in response to the MWCNT challenge.

Reduced PPARγ expression has downstream effects including increased NFκB activation. Therefore, we expect the sarcoidosis disease state and MWCNT murine model to promote the transcription of genes controlled by this factor including matrix metallopeptidase 12 (MMP12) and osteopontin (OPN). Each of these genes have been implicated in granuloma formation and have become a focus within this study of granuloma resolution (19).

1.7 Matrix metalloproteinase 12 is a key factor in granuloma formation

Matrix metalloproteinase-12 (MMP12) is a member of a family of extracellular endopeptidases. The molecule was first studied for its involvement in extracellular matrix remodeling. In recent years, however, MMPs have been implicated in immune functions including cell migration, leukocyte activation, and anti-microbial defense (29). MMP12 is one of the most upregulated genes in sarcoidosis patients and in the MWCNT murine model (20, 30). Studies have shown that expression is highest near active granulomatous inflammation and that

there is a correlation between protein levels and disease severity, suggesting that MMP12 contributes to inflammation and granuloma formation (31). The factor is known to facilitate the infiltration of immune cells (32) and its production by macrophages is induced by OPN, a cytokine that promotes cell adhesion and is a key factor in granuloma formation (19, 30). MMP12 knockout mice exhibit granuloma resolution 60-days post instillation with MWCNT, further suggesting that MMP12 is necessary for granuloma persistence (30).

1.8 Osteopontin promotes the structural integrity of granulomas

Osteopontin (OPN) is characterized as both a matricellular protein and a type 1 (Th1) cytokine. As a potent chemoattractant, the protein has been implicated in cell-mediated immune responses and is upregulated at sites of inflammation and tissue remodeling (33). OPN is produced by several types of immune cells including macrophages. Its relationship with macrophages is extensive as the protein is known to regulate macrophage migration, survival, phagocytosis, and pro-inflammatory cytokine production (33). The activity of OPN is regulated through post translational modifications (33-35). Proteolytic cleavage at its active thrombin cleavage site modulates the protein's function and its ability to bind to integrins (33, 34). This cleavage can be accomplished by MMPs, including MMP12 (34, 35). Post cleavage, integrins such as $\alpha_v\beta_{3,}$ can bind to RGD (arg, gly, asp) sequences, increasing cell adhesion (33).

OPN is one of the most highly expressed proteins in several lung diseases. It is prominent in pulmonary granulomas from human patients caused by tuberculosis, fungal infections, and sarcoidosis (34, 36). This cytokine has also been implicated in granuloma formation in murine models of granulomatous disease. Previous studies have shown

upregulation of mRNA expression and protein in MWCNT instilled mice (19). OPN deficient models are characterized by smaller lesions with less macrophage recruitment, indicating that OPN plays a role in macrophage accumulation in granulomatous structures (37). Current literature suggests that OPN is a key mediator in granuloma formation that promotes the migration of inflammatory cells to sites of injury and promotes cellular adhesion.

1.9 Proposed Mechanism of Granuloma Formation

Previous studies and current literature have provided evidence for a proposed mechanism of granuloma formation which was presented in the 2011 Huizar et al. study (Figure 1). The pathway emphasizes the roles of OPN and MMPs in the formation of granulomas. The mechanism suggests that an initial injury triggers alveolar macrophage secretion of cytokines including CCL2 and OPN which leads to further recruitment of alveolar macrophages and T cells (19). Macrophages produce MMPs, including MMP12, that alter cytokine signaling via proteolytic cleavage of OPN. OPN fragments bind to integrins, leading to macrophage transformation and increased cell adhesion molecules. The fusion of macrophages leads to the formation of giant cells. T cells are retained, leading to persistence of granulomatous inflammation and continued accumulation of immune cells (19).

1.10 Instillation of PPARγ-KO mice with MWCNT

Based on the observed PPARγ deficiency in sarcoidosis patients, it was hypothesized that the factor may play a role in MWCNT granuloma formation. This led to the examination of PPARγ expression and activity in C57BL/6J mice. The results revealed decreased expression

and activity in the MWCNT instilled model and prompted the use of a macrophage-specific PPARγ knockout strain to further uncover the effects of PPARγ deficiency on sarcoidosis pathophysiology (27).

Sixty days post instillation with MWCNT, the PPARγ knockout mice displayed exacerbated granuloma size compared to C57BL/6J mice. Gene expression and protein for cytokines CCL2, OPN, and IFNγ was increased (27). Granulomas in the knockout mice had significant fibrosis whereas the C57BL/6J mice did not. TGFβ protein, a potent driver of fibrosis, was elevated in MWCNT instilled PPARγ-KO mice compared to PBS controls, however, the protein was below detectable levels in C57BL/6J animals (38). The downstream protein, smad3, was also elevated in the PPARγ knockouts, indicating that upregulation of this pathway may be the source of increased fibrosis (38). Prior to the current study, the PPARγ knockout mice had not been evaluated 90-days post instillation.

1.11 Hypothesis

Prior studies have shown that 60-days post MWCNT instillation, macrophage specific PPARγ-KO mice exhibit more robust granuloma formation and fibrosis compared to C57BL/6J controls. We hypothesized that 90-days post instillation, PPARγ-KO mice would maintain extensive granulomatous inflammation and fibrosis.

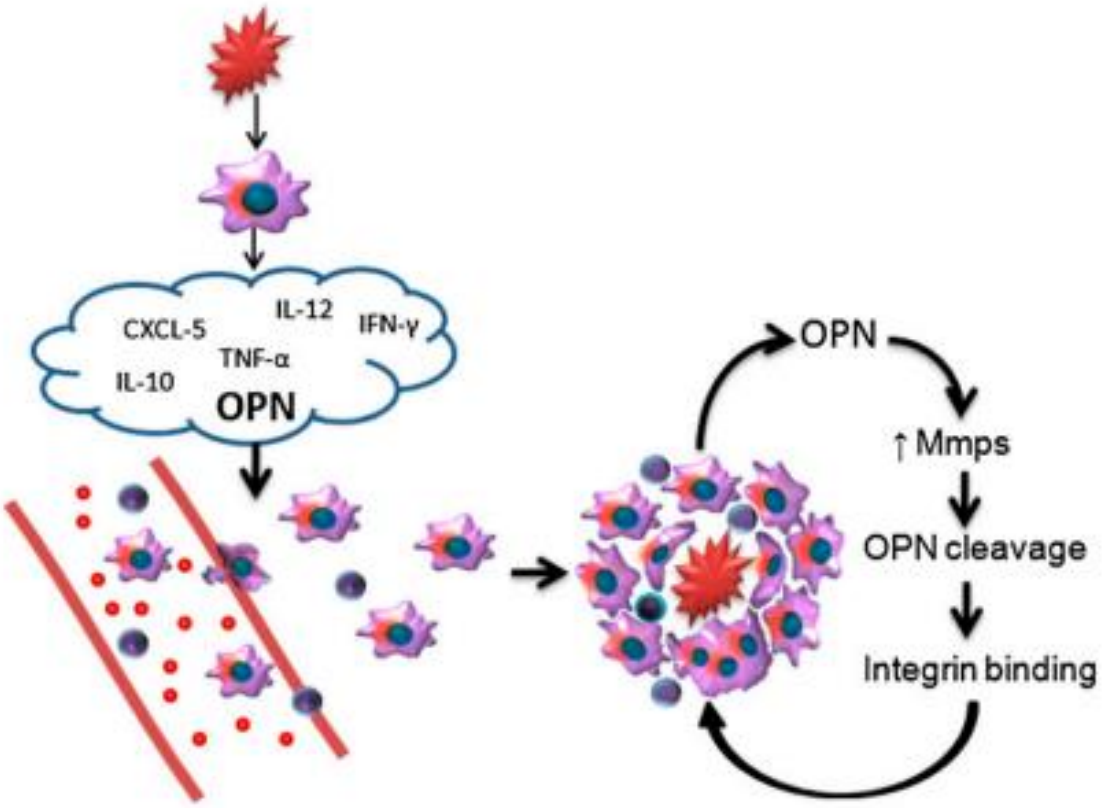

Figure 1. Proposed mechanism for granuloma formation. Initial injury triggers alveolar macrophage secretion of cytokines and further recruitment of alveolar macrophages and T cells. OPN induces production of MMP12. MMP12 alters OPN via proteolytic cleavage, increasing its cellular adhesion properties which promotes the persistence of granulomatous inflammation.

CHAPTER 2:

Materials and Methods

2.1 Mice

This study was conducted in conformity with Public Health Service (PHS) policy on humane care and use of laboratory animals. All experiments were approved by the institutional animal care committee (AUP #J199d). C57BL/6J and macrophage-specific PPARγ-KO mice were utilized. The C57BL/6J mice were obtained from The Jackson Laboratory (Bar Harbor, ME). Homozygous floxed (+/+) PPARγ mice were provided by Dr. F. J. Gonzalez (National Institutes of Health, Bethesda, MD). To achieve loss of PPARγ in macrophages, these animals were crossed with mice containing the cre recombinase transgene under the direction of the murine M lysozyme promoter from The Jackson Laboratory (39). The heterozygous mice were genotyped to generate the $\text{flox}^{+/+}/\text{cre}^{+/+}$(PPAR$\gamma$-KO) strain. Both C57BL/6J and PPARγ-KO strains were placed in breeding pairs at 7 weeks of age. Breeders were replaced every six months. Studies were conducted using multiple age-matched litters.

2.2 Instillation with MWCNT

Pulmonary granulomas were generated by oropharyngeal aspiration of 100 µg MWCNT (catalog number 900-1501, lot GS1802, SES Research, Houston, TX) in phosphate buffered saline (PBS)/35% surfactant solution (gift from Ony Inc, Amherst, NJ). Mice were instilled with one 100 µg dose in 50 µl PBS/surfactant after sedation with isoflurane. Control mice received PBS/surfactant solution alone. Mice were sacrificed with tribromoethanol (TBE) 60 or 90-days post instillation.

2.3 Lung tissue processing

Lung tissue from C57BL/6J and PPARγ-KO mice was embedded in paraffin or frozen in optimal cutting temperature (OCT) compound for future experimentation. Paraffin embedding was achieved by inflating the lungs with 300 µl of formalin and fixing the tissue overnight in PBS-buffered 10% formalin. After 24 hours, the tissue was moved to 70% ethanol before being submerged in paraffin. Lungs frozen in OCT were inflated with 300 µl of a 3:2 OCT and PBS solution. All tissue samples were placed into cassettes, covered in OCT, and flash frozen.

2.4 Histological assessment

Paraffin embedded lungs were cut into 5 µm sections and stained with either hematoxylin and eosin (H&E) or Gomori's Trichrome (College of Veterinary Medicine Histology Core at North Carolina State University, Raleigh, NC). Quantitative granuloma scoring was completed on H&E-stained slides as previously described (27). Representative images were taken for each strain, condition, and time point using an Axio Imager 1A (Zeiss, Oberkochen, Germany) .

2.5 Bronchoalveolar lavage (BAL)

Mice were sacrificed via intraperitoneal TBE injection. The tracheas were cannulated with plastic tubing and the lungs were lavaged with 1 ml aliquots of warm 0.2% lidocaine in PBS solution. This step was repeated 5 times. The resulting lavage was centrifuged at 1800 rpm for 10 minutes at 4 °C. Cytospins were produced by spinning 120 µl of cell suspension in a cytocentrifuge for 5 minutes at 500 rpm at room temperature and were stained with Diff Quick

Solution (Thermo Fisher Scientific, Waltham, MA). Differential counts were performed to determine the percent alveolar macrophages (AM), lymphocytes (Lym), and polymorphonuclear (PMN) cells in the population. Total cell counts were determined using a hemocytometer. Cells were centrifuged and resuspended once before differential counts and a second time before aspiration and storage at -80 °C.

2.6 Immunostaining of lung tissue and BAL cells

Immunofluorescent staining for MMP12 and OPN was performed on cryosectioned lung tissue frozen in OCT and on cytospins of freshly isolated BAL cells. Experiments were completed for all strains, conditions, and timepoints. All samples were fixed with 4% paraformaldehyde and permeabilized with 0.1% Triton-X-100. Tissue sections and BAL cells were stained for monoclonal Ms αMMP12 (1:250) (sc-390863, Santa Cruz Biotechnology, Dallas, TX) and monoclonal Ms αOPN [(1:100 tissue); (1:250 BAL cells)] (sc-21742, Santa Cruz Biotechnology, Dallas, TX). Samples were incubated overnight at 4 °C. After washing 3x with PBS, Alexa 488 F(ab)2 goat anti-mouse 2° antibody 1:1000 (Life Technologies, Carlsbad, CA) was applied. Slides were counterstained with DAPI to facilitate nuclear localization. Images were taken using a LSM 700 confocal microscope (Zeiss, Oberkochen, Germany).

2.7 Analysis of bronchoalveolar lavage fluid

MMP12 and OPN proteins were evaluated using the Mouse MMP-12 ELISA Kit (ab246540, Abcam, Cambridge, MA) and the Mouse/Rat Osteopontin Quantikine ELISA Kit

(MOST00, R&D Systems, Minneapolis, MN) respectively according to the manufacturer's instructions.

2.8 RNA purification and analysis

Total RNA was isolated from BAL pellets using miRNeasy kits (Qiagen, Germantown, MD). cDNA was produced using a RT2 First Strand Kit (Qiagen, Germantown, MD). Relative mRNA expression levels were computed using either a StepOnePlus PCR System (Thermo Fisher Scientific, Waltham, MA) or a QuantStudio 3 PCR System (Thermo Fisher Scientific, Waltham, MA). All samples were run in duplicates. Glyceraldehyde 3-Phosphate Dehydrogenase (GAPDH), a housekeeping gene, was used for comparison to determine ΔCt values. Data points are represented as dCT values. Increased dCT values represent decreased gene expression and vice versa. See the appendix section for a list of primers used in this manner.

2.9 Statistical analysis

Data were analyzed by either two-way Student's t test or by two-way ANOVA with Tukey's multiple comparisons test. Prism 7 software (GraphPad Inc., San Diego, CA) was used in all cases.

CHAPTER 3:

Fibrosis attenuation at 90-days post instillation with MWCNT in the PPARγ-KO strain does not appear to be associated with the canonical TGFβ pathway

RESULTS:

3.1 Granuloma size and fibrotic severity is decreased in PPARγ-KO mice 90-days post instillation compared to 60-day.

Previous studies have shown that instillation with MWCNT produces a granulomatous inflammatory response in both C57BL/6J and PPARγ-KO mice. In the C57BL/6J mice, granulomatous lesions are first evident 10-days post instillation, though the structures are small and poorly formed. At 60-days, well-formed granulomas with MWCNT aggregates are found. These structures remain present 90-days post instillation (19). PPARγ-KO mice are characterized by exacerbated granuloma formation at the 60-day time point compared to C57BL/6J mice, indicating a greater inflammatory response (27). Prior to this study, the PPARγ-KO strain had not been evaluated 90-days post instillation.

Given that PPARγ is a negative regulator of pro-inflammatory macrophage activation (25), we expected PPARγ-KO granulomatous lesions to remain large and well-formed 90-days post instillation. Surprisingly, granulomas were attenuated at 90-days compared to their 60-day counterparts (Figure 1A). These histological observations were quantified using a scoring system that takes granuloma size and frequency into account. As expected, granuloma scores in C57BL/6J tissue were similar at both timepoints. Both 60 and 90-day tissue samples had granuloma scores of 1-2 (Figure 1B). PPARγ-KO lung scores were higher than those of C57BL/6J at 60-days, receiving scores between 3-5, repeating previous findings (38) (Figure 1B). At 90 days, PPARγ-KO granuloma sizes were reduced compared to those at 60 days with scores between 1-2 (Figure 1B). These results corroborate the qualitative data.

In addition to granuloma size, we investigated fibrotic severity in granulomatous regions at both timepoints. Previous studies have shown that PPARγ-KO mice display significantly

more fibrosis at 60-days compared to C57BL/6J mice (38). Our results confirmed this finding at 60-days though by 90-days post instillation fibrosis was attenuated (Figure 2). Low levels of fibrosis were observed in C57BL/6J mice at both timepoints (Figure 2).

3.2 The canonical TGFβ signaling pathway does not appear to the be the source of fibrosis attenuation in PPARγ-KO mice at 90-days post instillation.

Histological data reveals that in addition to granuloma resolution, the PPARγ-KO strain has decreased fibrosis surrounding the granulomatous lesions at 90-days post instillation. This finding initiated an exploration of TGFβ, a well-studied profibrotic mediator. We were especially interested in TGFβ because studies have shown that it is upregulated in cells from human sarcoidosis patients compared to healthy controls (40). Previously, our lab has shown that TGFβ is increased in MWCNT-exposed PPARγ-KO mice at 60-days post instillation compared to PBS instilled controls (38). This result led to the hypothesis that TGFβ contributes to the observed increase in fibrosis at 60-days in the PPARγ-KO strain and may be involved in the attenuation at 90-days.

In the current study, TGFβ gene expression and protein were assessed in conjunction with gene expression of two downstream mediators in the canonical TGFβ signaling pathway, Smad3 and Smad7. Smad3 is a receptor activated transcription factor that is phosphorylated by TGFβ. Once activated, it dimerizes and translocated to the nucleus to affect the transcription of profibrotic genes. Smad7 is an inhibitory factor that antagonizes TGFβ signaling through binding to TGFβ and inhibiting the phosphorylation of Smad3 (41).

Our results confirm that TGFβ protein is increased in the MWCNT condition at 60-days ($p = 0.0068$) and show that protein levels are further increased at the 90-day timepoint ($p = 0.0318$) (Figure 3A). TGFβ gene expression data, however, is decreased at 90-days compared to PBS controls ($p = 0.0119$) (Figure 3B). There is a slight decrease but not a significant difference between the MWCNT gene expression at 60 and 90-days. Further qPCR analyses did not reveal changes between the 60 and 90-day MWCNT conditions for Smad3 and Smad7 (Figure 3C; Figure 3D). Taken together, these results do not suggest that the canonical TGFβ pathway is the source of fibrosis attenuation surrounding the granulomatous regions in the PPARγ-KO strain at 90-days post instillation with MWCNT.

DISCUSSION:

Instillation with MWCNT produces a granulomatous inflammatory response in both C57BL/6J and PPARγ-KO mice. In C57BL/6J mice, well-formed granulomas are evident by 60-days post instillation. These structures persist at 90-days (19). Given that PPARγ is a negative regulator of pro-inflammatory macrophage activation, we hypothesized that granulomatous inflammation in PPARγ-KO mice instilled with MWCNT would persist to 90-days post instillation. Surprisingly, the mice at the 90-day timepoint were characterized by poorly formed, small granulomas in contrast to those harvested 60-days post instillation. Additionally, while fibrosis accumulation is observed in 60-day MWCNT instilled mice, the 90-day timepoint revealed attenuated fibrosis. These findings led to further investigation with the PPARγ-KO mice at 90-days post instillation to determine key factors involved in the resolution of granulomatous structures and fibrosis.

We began by looking at the canonical TGFβ pathway, a well-studied mechanism of fibrogenesis. Gene expression from PPARγ-KO BAL cells revealed decreased TGFβ expression at 90-days when fibrosis is decreased. However, downstream mediators, Smad3 and Smad7, were unchanged between the 60 and 90-day MWCNT conditions. These findings lead us to believe that the canonical TGFβ pathway may not be responsible for the observed change. Contrary to the gene expression data, results from a TGFβ ELISA assay on BAL fluid revealed that TGFβ protein is elevated in MWCNT conditions at 60 and 90-days compared to PBS controls. 90-day MWCNT levels were significantly higher than those at 60-days. This data does not support the gene expression results. Because BAL fluid is composed of soluble compounds

from a variety of cell types, including epithelial cells, it is likely that the increased TGFβ content is not from the macrophages, the key drivers of granulomatous formations.

TGFβ and the Smad family of protein's role in fibrogenesis is widely recognized, however Smad-independent pathways have been implicated in the pathogenesis of fibrosis in lung tissue (41, 42). Mediators in these pathways include c-Abi kinase and Erk1/2 (41-43). Future studies could evaluate factors in these alternative pathways to determine their involvement in the reduction of fibrosis at 90-days post instillation in the PPARγ-KO strain.

Fibrosis is the result of fibroblast activation and subsequent ECM deposition (44). Pulmonary fibrosis is a result of several diseases including sarcoidosis and idiopathic pulmonary fibrosis (IPF). IPF is a progressive disease that causes scar tissue build up in the lungs, impairing lung function. There are several differences between the fibrosis observed in sarcoidosis and IPF. Sarcoidosis affects younger populations, has a lower mortality rate, and is characterized by fibrosis found predominantly in the upper lobe (44). IPF affects older patients, has a higher mortality rate, and causes fibrosis in peripheral regions and in the lower lobe of the lung (44). Despite these differences, both sarcoidosis associated fibrosis and that caused by IPF are widely believed to be irreversible (44-46).

Several animal models of pulmonary fibrosis have been developed in addition to our MWCNT model. The most widely studied model of IPF is the bleomycin model in which bleomycin causes pulmonary inflammation and fibrosis after intratracheal or intravenous instillation (47). A limitation of this model is that fibrosis resolves within three weeks (47). This is true for most models of pulmonary fibrosis; however, the degree of reversibility is not uniform (48). Models with more intense fibrotic triggers and prolonged exposure have less fibrosis attenuation (48, 49). The mechanism of this reversal is unknown; however, factors with possible

involvement are currently under evaluation. Three areas of current research include proteolytic degradation of the ECM including collagen types I and III, inhibition of myofibroblast differentiation, and the role that macrophage polarization plays in fibrosis reversal (48). M2 macrophages are associated with fibrotic remodeling (50). Future experiments should evaluate the BAL cell population in C57BL/6J and PPARγ-KO mice at 60 and 90-days post instillation to determine if changes in macrophage phenotype occur as fibrosis decreases.

Current literature describes human pulmonary fibrosis observed in diseases such as sarcoidosis and IPF as irreversible (44-46). However, fibrosis attenuation occurs in several animal models (48) including our PPARγ-KO mice at 90-days. The mechanism of this reversal is not well understood and is the topic of many current studies. Further research is required to understand how fibrosis in animals is achieved and if it can elucidate factors for therapeutic reversal of fibrosis in human patients.

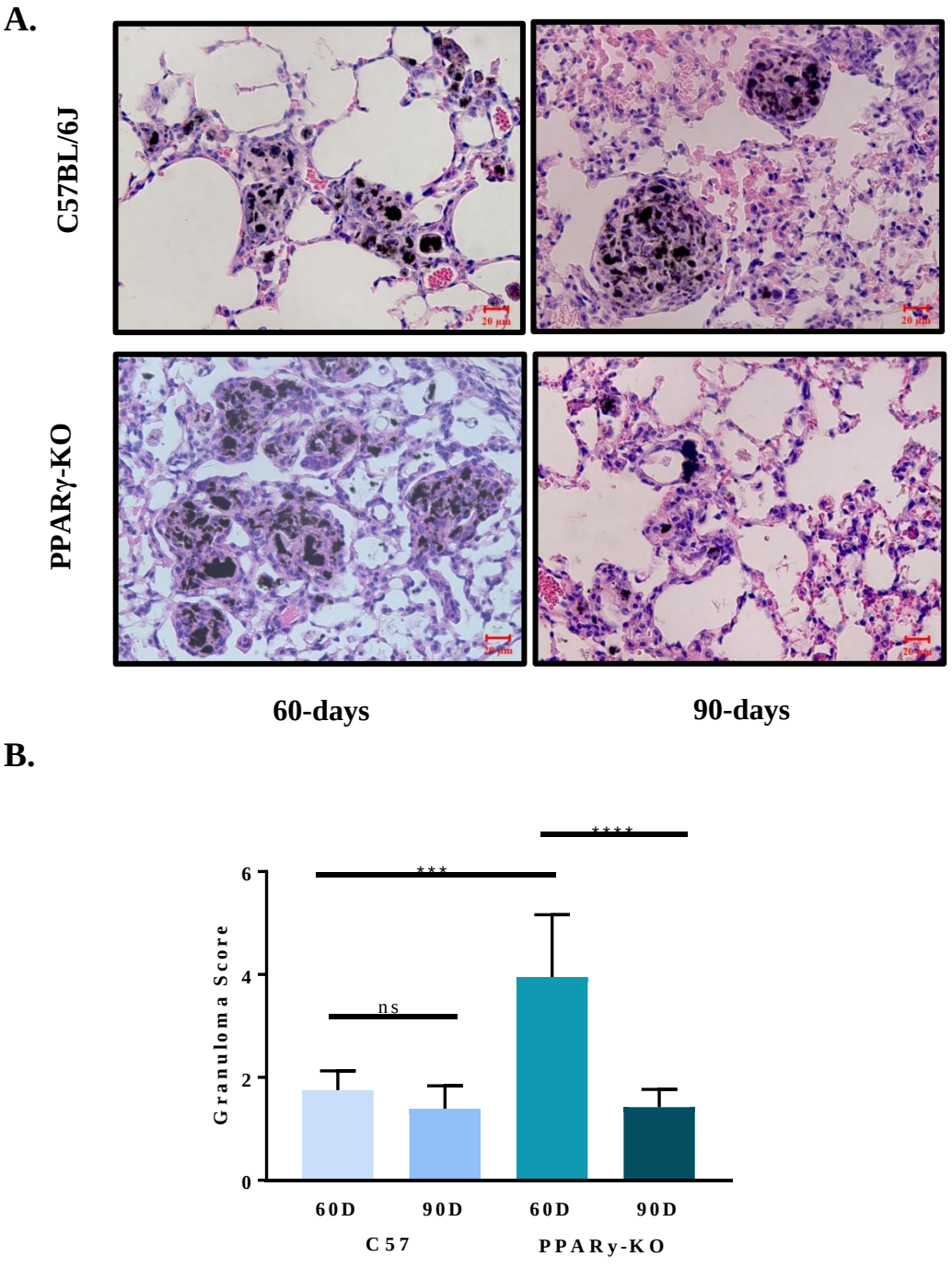

Figure 1. Granuloma size is decreased in PPARγ-KO mice 90 days post instillation compared to 60-days and C57BL/6J mice. (A) Lung sections from 60 and 90-day C57BL/6J and PPARγ-KO mice treated with MWCNT were stained with H&E. Representative images are shown for each strain and timepoint at 40X magnification. Qualitative analysis was completed on n ≥ 6 per group. **(B)** Granuloma scoring for C57BL/6J and PPARγ-KO strains at 60 and 90-days post instillation. Data is represented as mean ± SEM for n ≥ 8 per group; *** and **** represent $p < 0.001$ and $p < 0.0001$ respectively by Student's t-test.

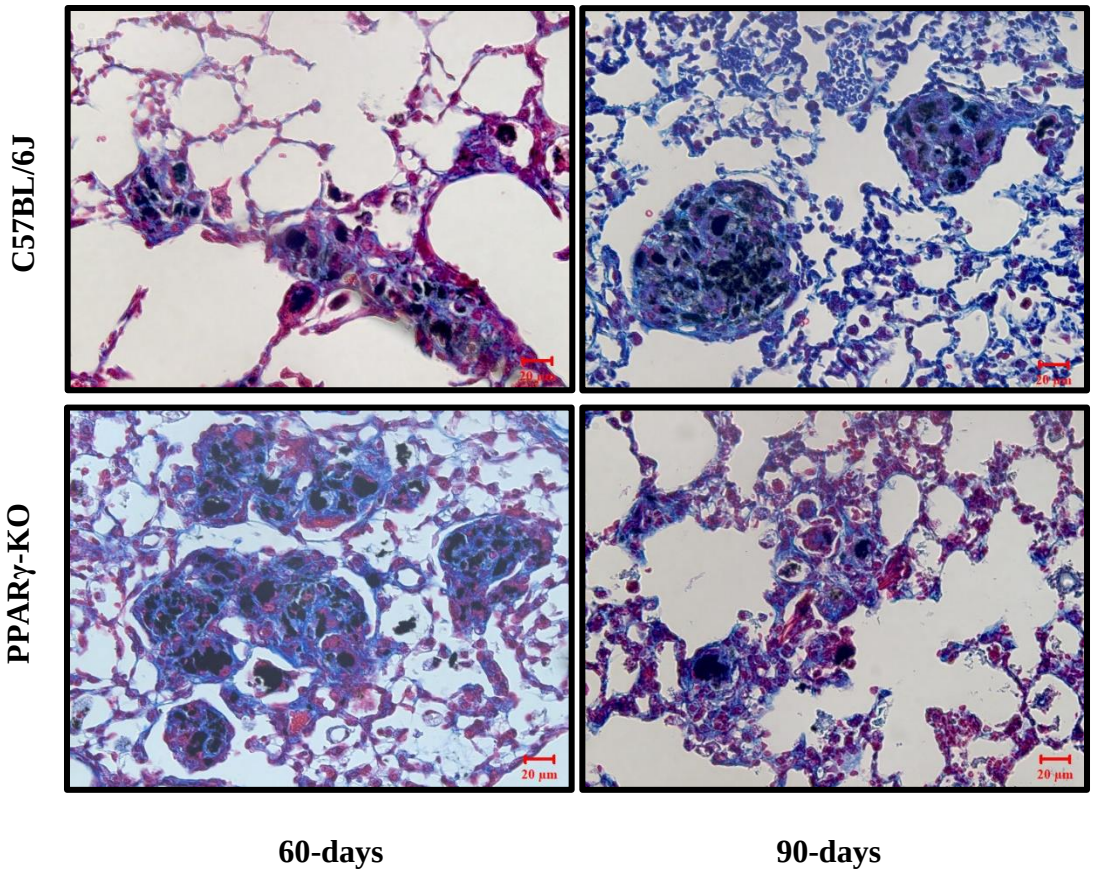

Figure 2. PPARγ-KO mice display exacerbated fibrosis 60-days post instillation and attenuated fibrosis at 90-days. Lung sections from 60 and 90-day C57BL/6J and PPARγ-KO mice treated with MWCNT were stained with Gomori's trichrome for collagen (stained blue). Representative images are shown for each strain and timepoint at 40X magnification. Qualitative analysis was completed on $n \geq 6$ per group.

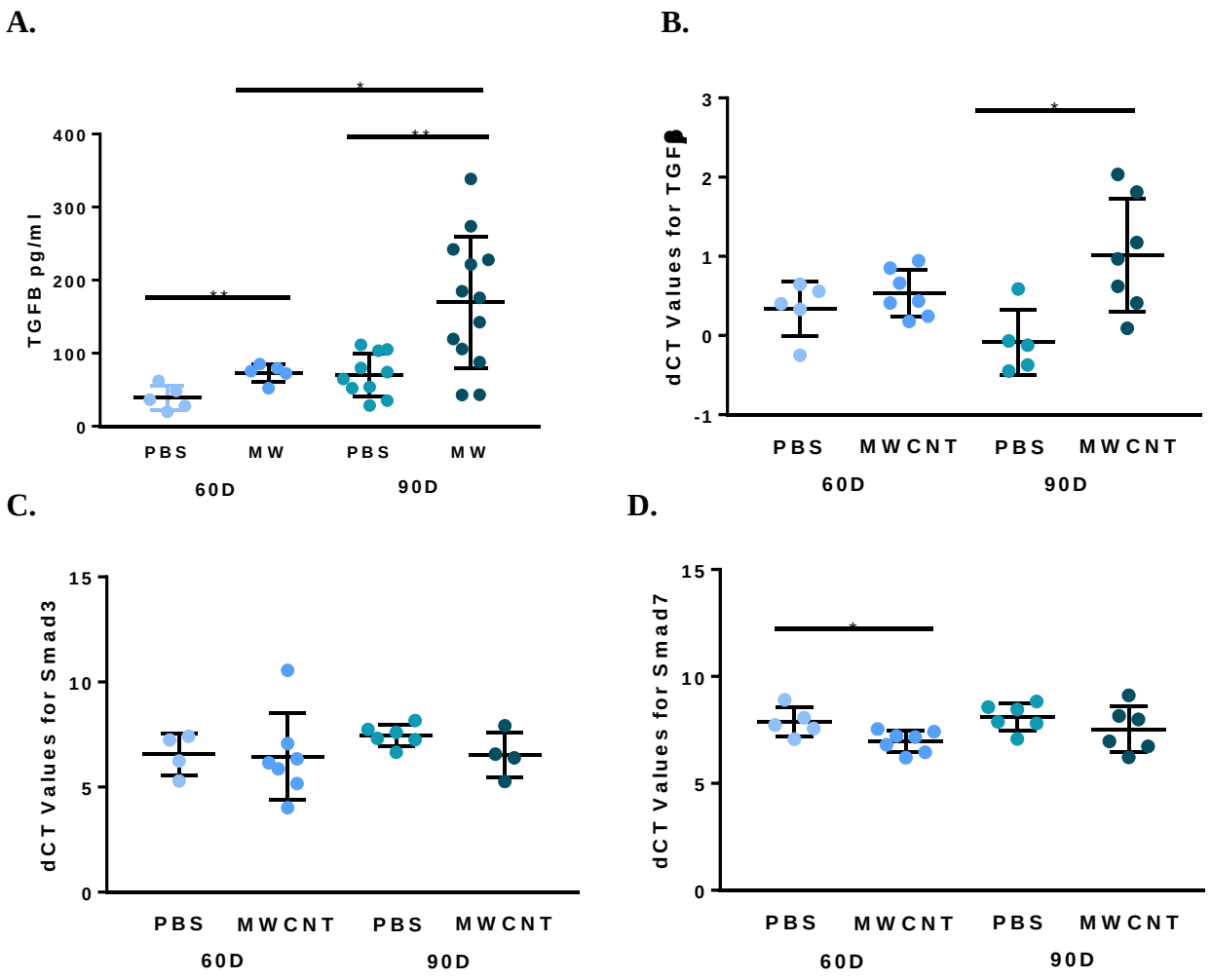

Figure 3. Decreased fibrosis in the PPARγ-KO model at 90-days is not associated with decreased expression of mediators implicated in canonical TGFβ signaling. A). TGFβ protein in BAL fluid from PPARγ-KO mice 60 and 90-days post instillation. Gene expression from PPARγ-KO BAL cells for (B) TGFβ, (C) SMAD3, and (D) SMAD7. Data is represented as mean ± SEM for n = 4-11 per group. * and ** represent $p < 0.05$ and $p < 0.01$ respectively by Student's t-test. (Data points are represented as dCT values. Increased dCT values represent decreased gene expression and vice versa.)

CHAPTER 4:

MMP12 and OPN protein is decreased in PPARγ-KO tissue 90-days post instillation with MWCNT compared to 60-days

RESULTS:

4.1 MMP12 and OPN is decreased in 90-day MWCNT exposed PPARγ-KO lung tissue compared to 60-day.

Matrix Metalloproteinase-12 (MMP12) is a member of a family of extracellular endopeptidases. The protein is involved in macrophage activation and plays a role in the regulation of inflammation through interactions with cytokines (32, 33). Osteopontin (OPN) is a cytokine and potent chemoattractant that has been implicated in cell-mediated immune responses (33). OPN has been shown to regulate several macrophage functions including migration, survival, and pro-inflammatory cytokine production (33). The activity of OPN is regulated through post translational modifications (35).

MMP12 is known to cleave OPN, enhancing its cellular adhesion properties, which promotes the growth and persistence of granulomatous lesions (33-35). Previous work from our laboratory has implicated MMP12 and OPN as important factors in granuloma formation in the MWCNT murine model of sarcoidosis (19). Upon the observation of granuloma resolution in the PPARγ-KO strain at 90-days post instillation with MWCNT, we investigated these two factors through a time course study. At 60 and 90-days post instillation of PPARγ-KO mice with PBS or MWCNT, we assessed gene expression from BAL cells, protein in BAL fluid, and performed immunocytochemistry on BAL cells and tissue sections.

qPCR analyses indicated that both MMP12 (Figure 1A) and OPN (Figure 1B) gene expression increases in the 60 and 90-day MWCNT conditions compared to PBS controls. MMP12 expression decreases between the 60 and 90-day MWCNT conditions ($p = 0.0002$) (Figure 1A). This is not observed for OPN. MMP12 and OPN ELISA assays on BAL fluid support

the qPCR finding and show that both proteins are increased in the 60 and 90-day MWCNT conditions compared to PBS controls (Figure 2A, Figure 2B). OPN protein is decreased in MWCNT instilled 90-day samples compared to the 60-day MWCNT condition ($p = 0.033$) (Figure 2B). This is not observed for MMP12.

Immunocytochemistry was performed on BAL cells collected by cytospins and were stained separately with antibodies to MMP12 and OPN. Representative images reveal that cells from 60-day PBS and MWCNT instilled PPARγ-KO express similar levels of MMP12 (Figure 3). An increase in MMP12 protein is observed between the PBS and MWCNT instilled groups at 90-days (Figure 3). Greater fluorescence is observed in 90-day MWCNT BAL cells when compared to 60-day MWCNT samples (Figure 3). The results from OPN BAL cell staining is similar to MMP12 staining. OPN is increased in the 60-day and 90-day MWCNT conditions compared to their PBS controls (Figure 4). As observed with MMP12, the 90-day MWCNT condition has increased OPN expression compared to the 60-day MWCNT group (Figure 4).

Lung sections from PPARγ-KO samples were subjected to immunohistochemistry. Sixty and 90-day PBS and MWCNT instilled sections were stained separately with antibodies to MMP12 and OPN. Both MMP12 (Figure 5) and OPN (Figure 6) increased in the 60-day MWCNT conditions compared to 60-day PBS controls. At the 90-day timepoint, MMP12 fluorescence is unchanged between PBS and MWCNT instilled mice (Figure 5). When stained with OPN, 90-day tissue reveals decreased OPN expression in the MWCNT condition compared to PBS (Figure 6). Interestingly, both MMP12 and OPN is decreased in MWCNT at 90-days when compared to 60-day MWCNT instilled tissue (Figure 5; Figure 6). This result suggests that MMP12 and OPN both play a role in granuloma resolution at 90-days in the PPARγ-KO strain as granulomas persist and

resolve within pulmonary tissue. Table 1 provides a summary of the changes in MMP12 and OPN gene expression and protein in PPARγ-KO mice between the 60 and 90-day MWCNT conditions.

DISCUSSION:

Our observation that granulomas resolve in MWCNT instilled PPARγ-KO mice 90-days post instillation, lead to a study of MMP12 and OPN in effort to understand the mechanism responsible for the decreases in granulomatous inflammation. Because the observed differences take place between the 60 and 90-day MWCNT PPARγ-KO mice, we focused our experiments within the PPARγ-KO mice to investigate potential drivers of granuloma resolution. Table 1 summarizes the findings.

MMP12 gene expression in MWCNT-exposed PPARγ-KO BAL cells is decreased at 90-days compared to 60-days in BAL cells. Protein levels in the BAL fluid are unchanged between the timepoints. OPN gene expression is unchanged in the BAL cells between the two conditions, however, protein in the BAL fluid is decreased at 90-days. Interestingly, we observe increases in both MMP12 and OPN at 90-days when immunocytochemistry is performed on BAL cells. Contrary to our findings from the BAL cell staining, MMP12 and OPN protein is decreased in MWCNT-instilled lung tissue sections at 90-days compared to 60-days. This result suggests involvement in the resolution of granulomas at 90-days post instillation. This finding in tissue sections is especially important as pulmonary granulomas form and resolve within lung tissue.

Increased MMP12 and OPN in BAL cells at 90-days post instillation was an unexpected result. It is possible that the macrophages are working to clear the proteins at this timepoint when granulomas are resolving, which could explain the increases. Future experimentation at 120-days post instillation could provide insight. If protein levels are decreased at this timepoint in the BAL cells, it could indicate that there is a change in macrophage phenotype as macrophage polarization in response to specific microenvironments is known to alter function. BAL cells should be assessed for markers of M1, M2, and further subtyped macrophage populations to determine if a

change in phenotype occurs. It is also possible that the protein detected in the BAL cells is inactive. Future studies should be performed to assess OPN and MMP12 activity.

While further research is necessary to understand the mechanism behind the increased expression of MMP12 and OPN in BAL cells and their decreased expression in tissue, the fact that their expression follows the same trend suggests that they may work together to resolve granulomas. As mentioned previously, OPN is activated through post translational modifications (33-35). MMP12 is known to cleave OPN, regulating its role in cell-mediate immune responses and tissue remodeling (34, 35). Future studies are necessary to define the mechanism of action for the two proteins and assessing if protein in BAL cells is active. This could be aided by assessing the levels of cleaved OPN in BAL cells and tissue to determine OPN activity, which can be accomplished through immunostaining. Zymography assays could be employed to assess MMP12 activity. Such studies may clarify the relationship between MMP12 and OPN and their role in granuloma resolution in PPARγ-KO mice 90-days post instillation with MWCNT.

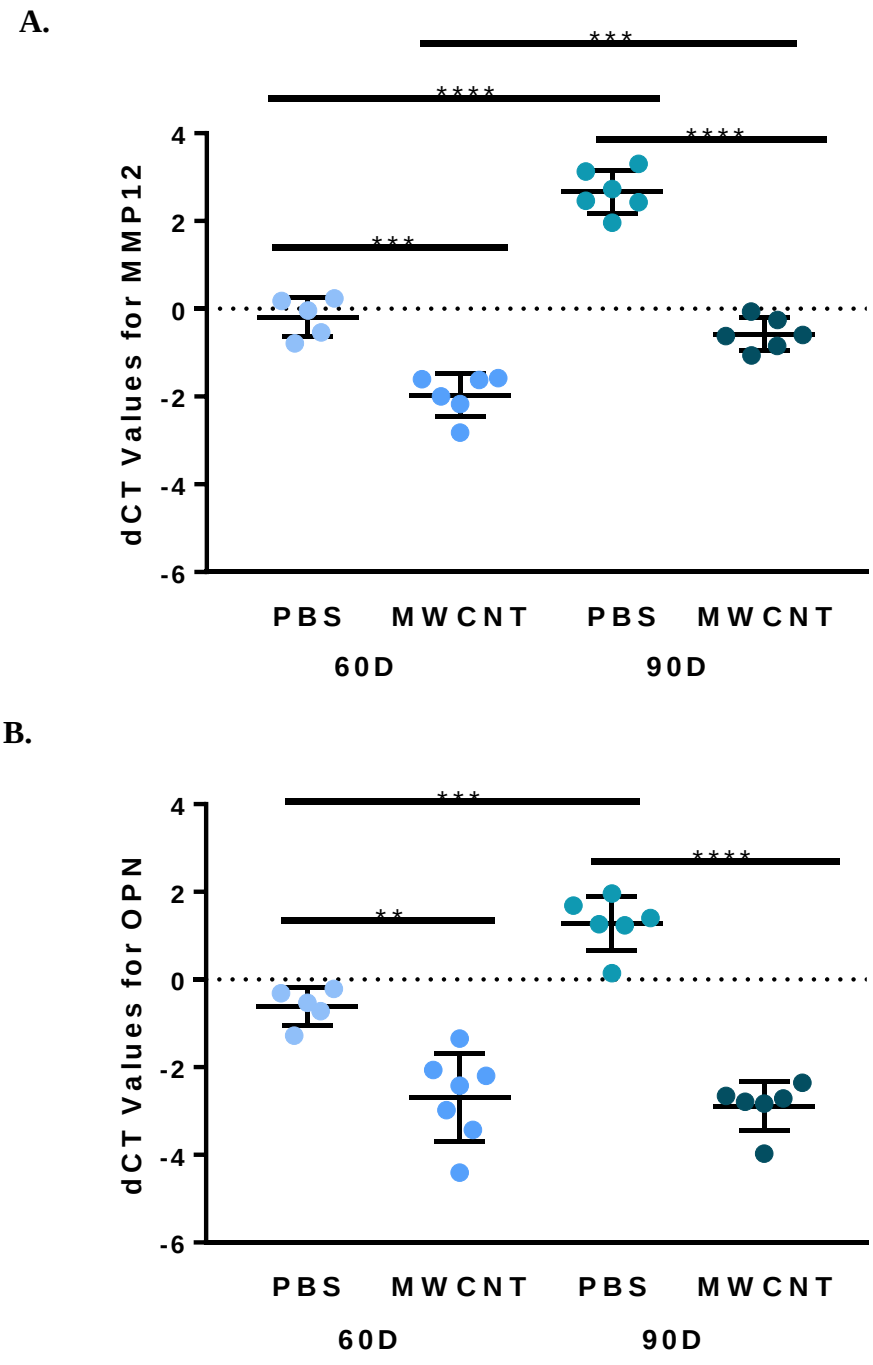

Figure 1. MMP12 gene expression is decreased in MWCNT challenged PPARγ-KO BAL cells at 90-days post instillation compared to those at 60-days. qPCR analysis of (A) MMP12 and (B) OPN in BAL cells from **PPARγ-KO** mice 60 and 90-days post instillation with PBS or MWCNT. Data is represented by mean dCT ± SEM for n ≥ 5 per group; **, ***, and *** represents $p \leq 0.01$, $p \leq 0.001$, and $p \leq 0.0001$ respectively by Student's t-test. (Data points are represented as dCT values. Increased dCT values represent decreased gene expression and vice versa.)

A.

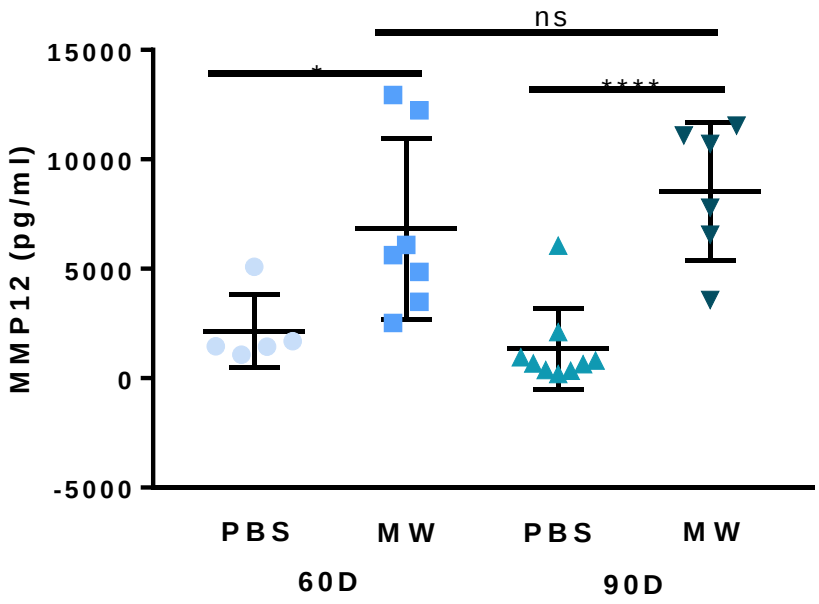

B.

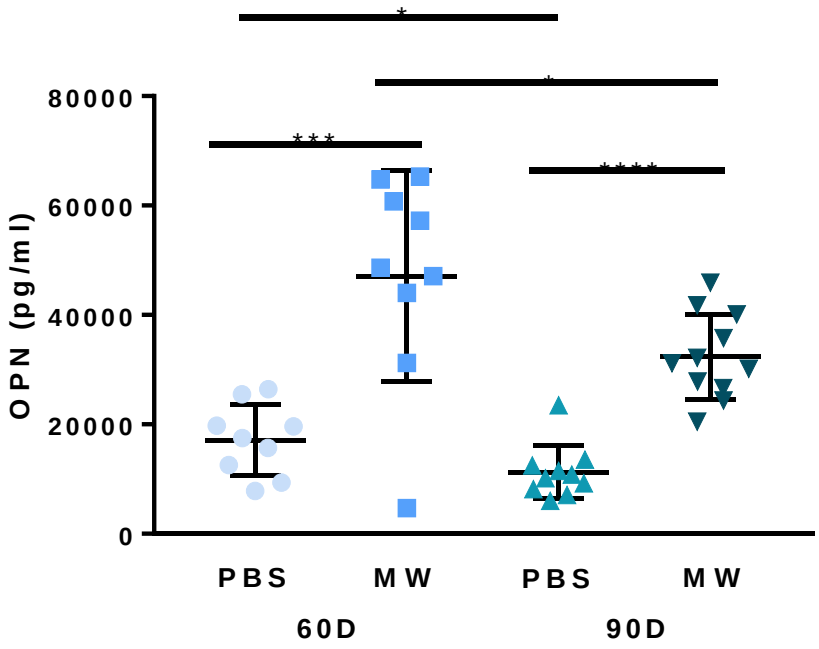

Figure 2. OPN protein is decreased in 90-day BAL fluid from MWCNT-instilled PPARγ-KO mice compared to 60-day. Analysis of (A) MMP12 and (B) OPN proteins in BAL fluid collected from PBS and MWCNT instilled PPARγ-KO mice 60 and 90-days post instillation. Data is represented by mean ± SEM for n ≥ 5 per group; *, ***, and **** represents $p \leq 0.05$, $p \leq 0.001$, and $p \leq 0.0001$ respectively by Student's t-test.

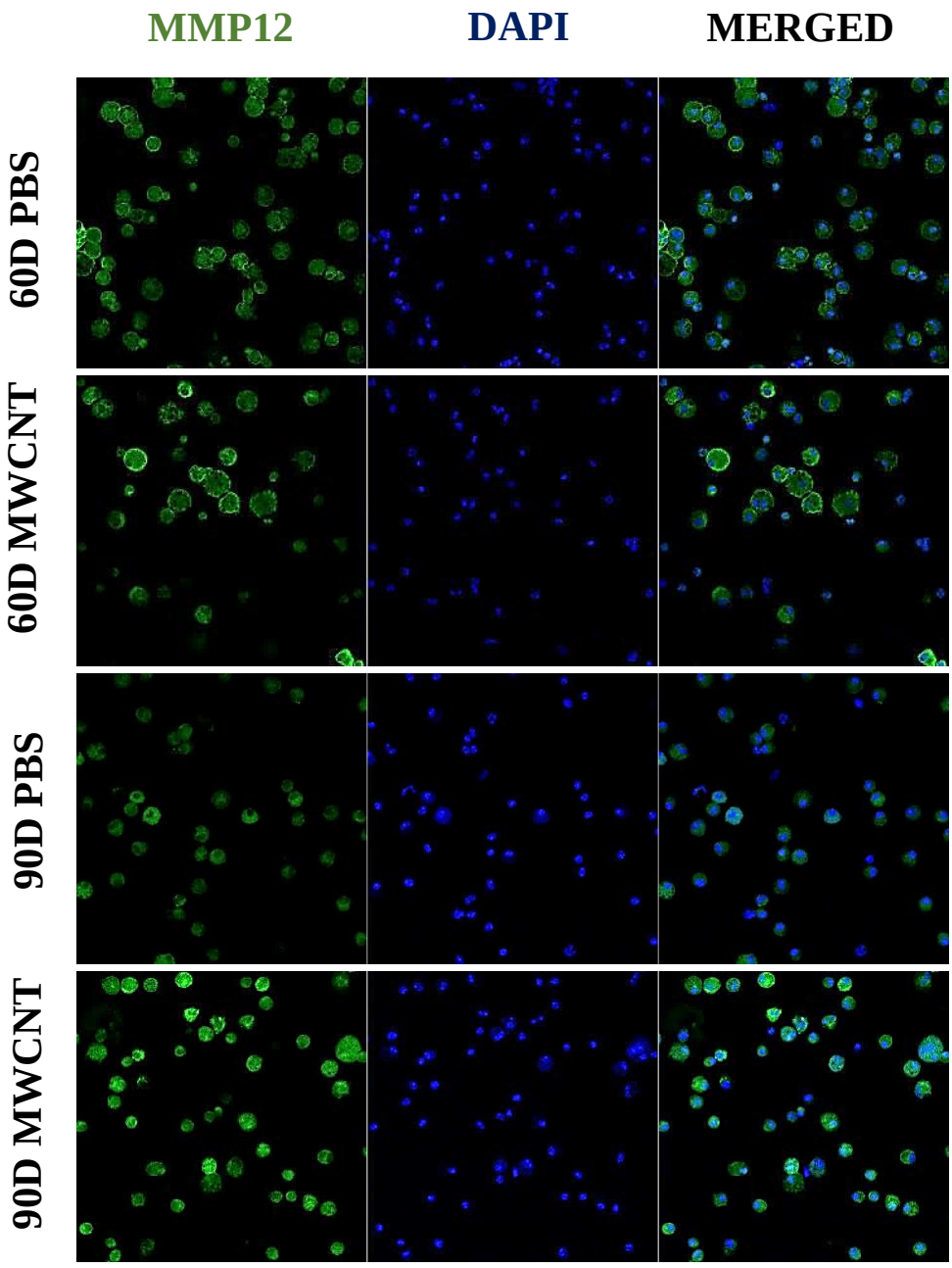

Figure 3. MMP12 protein is increased in BAL cells from MWCNT PPARγ-KO mice 90-days post instillation compared to 60-days. Immunocytochemistry was performed on BAL cells collected by cytospins. Cells were stained with antibody to MMP12 and counterstained with DAPI to localize nuclei. Qualitative analysis was completed on $n \geq 3$ per PBS group and $n \geq 4$ for MWCNT groups. Representative images are shown for each treatment and timepoint at 20X magnification.

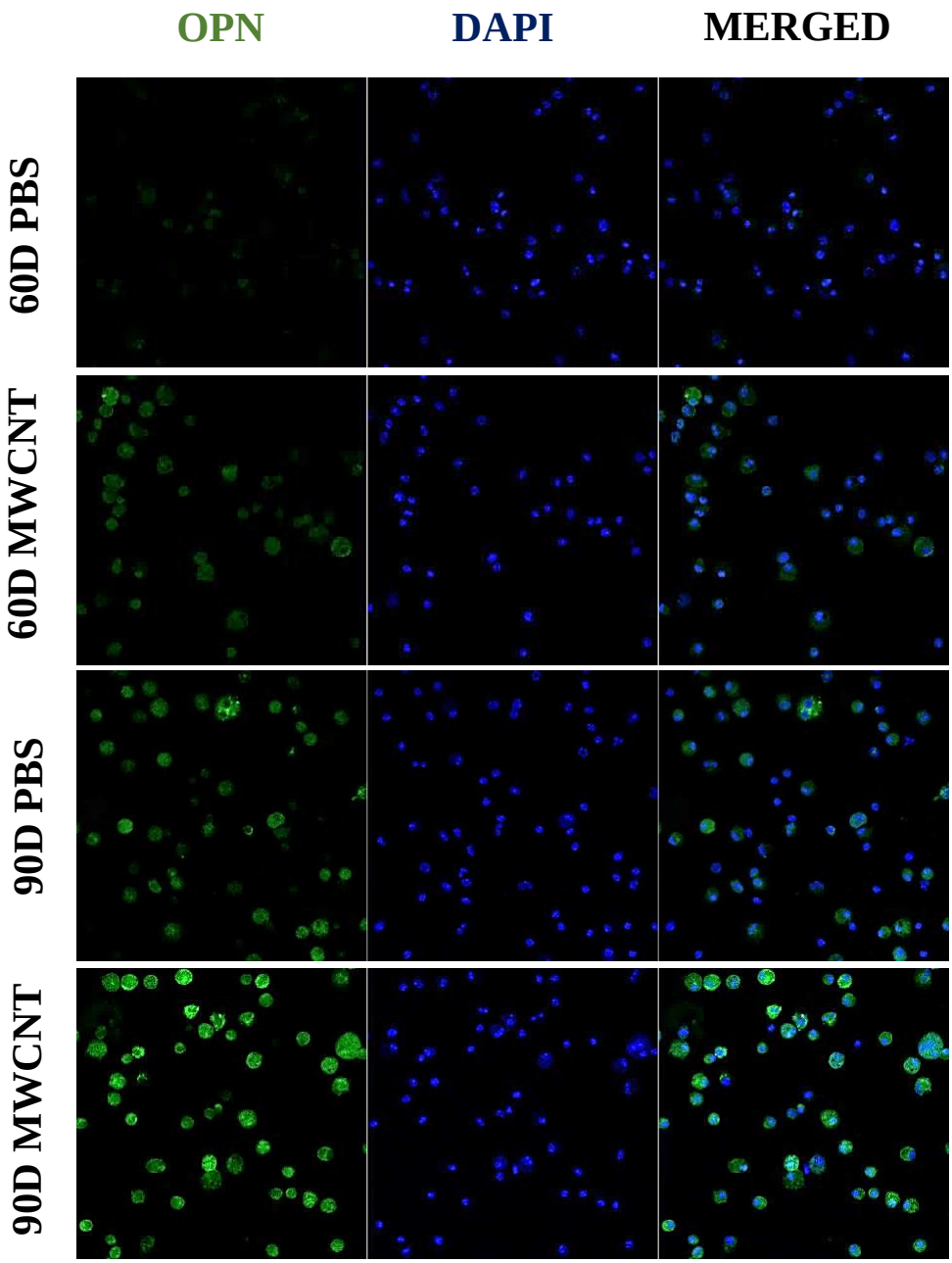

Figure 4. Immunocytochemistry on BAL cells reveal increased OPN protein in MWCNT instilled PPARγ-KO mice 90-days post instillation. BAL cells were collected by cytospins and stained with antibody to OPN. Slides were counterstained with DAPI to localize nuclei. Qualitative analysis was completed on $n \geq 3$ per PBS group and $n \geq 4$ for MWCNT groups. Representative images are shown for each treatment and timepoint at 20X magnification.

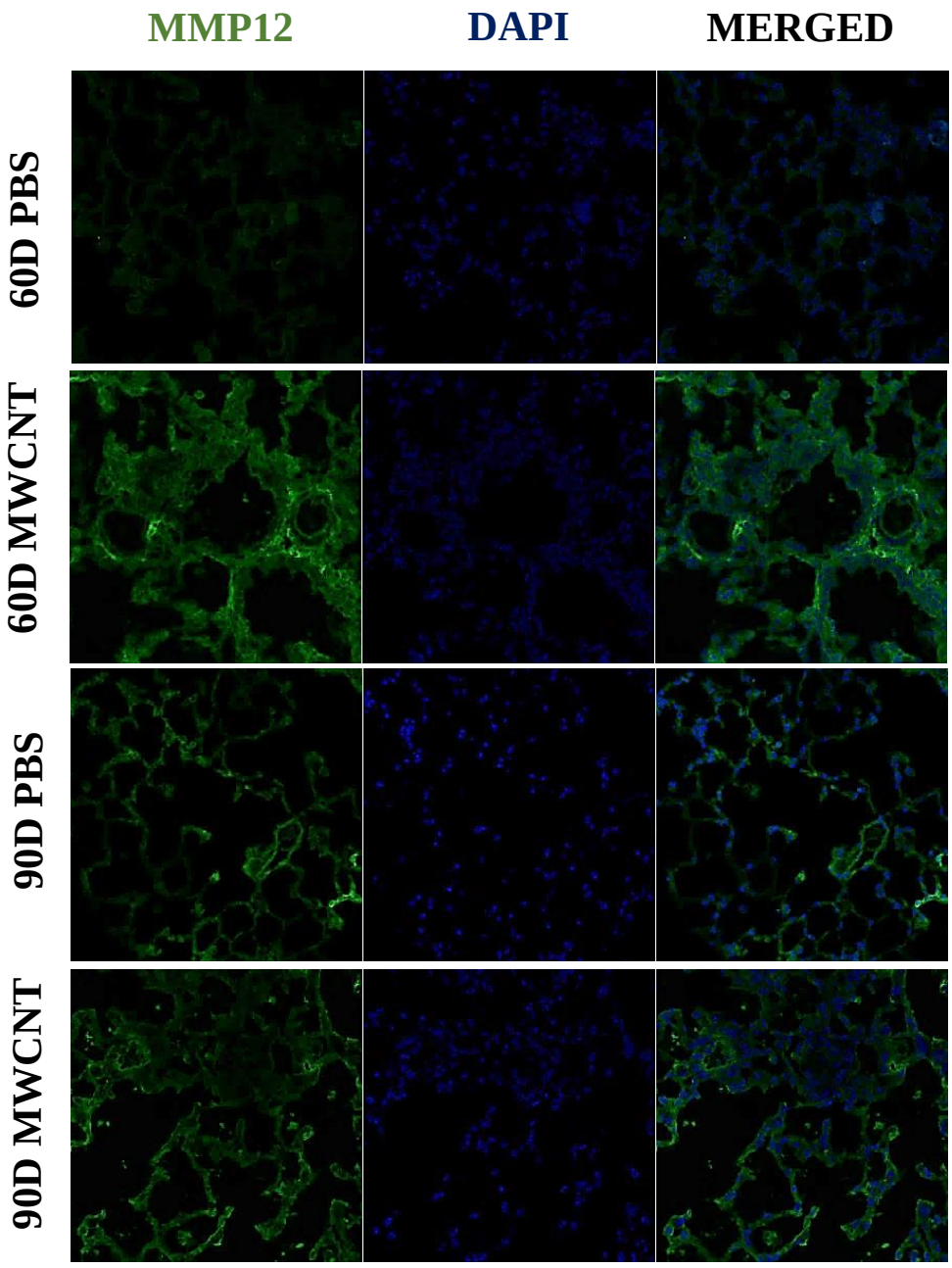

Figure 5. PPARγ-KO granulomatous tissue contains elevated MMP12 protein 60-days post instillation and decreased MMP12 protein at 90-days. Lung sections from 60 and 90-day PBS and MWCNT instilled PPARγ-KO mice were stained with antibody to MMP12 and counterstained with DAPI to localize nuclei. Qualitative analysis was completed on $n \geq 3$ per PBS group and $n \geq 4$ for MWCNT groups. Representative images are shown for each treatment and timepoint at 20X magnification.

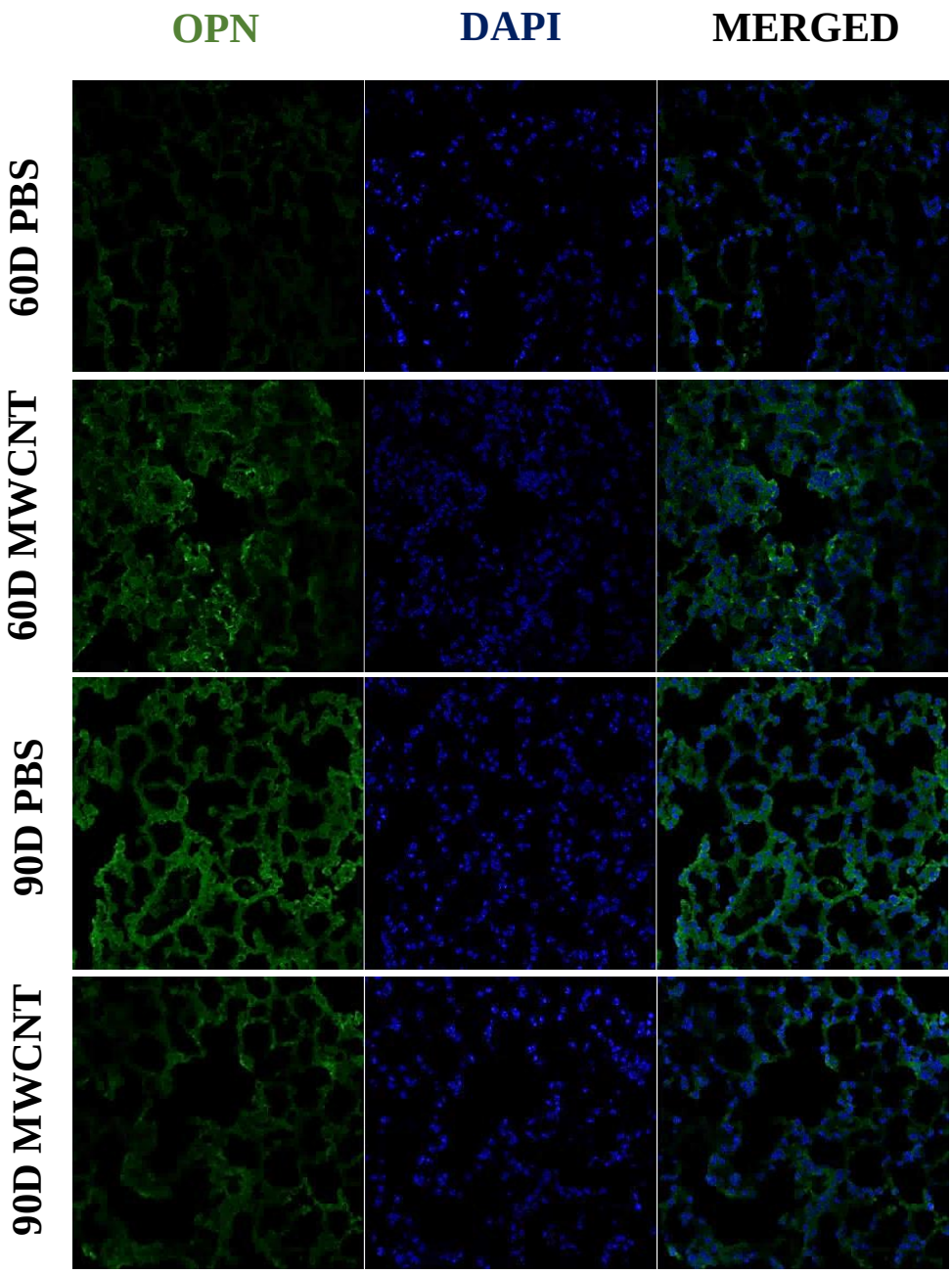

Figure 6. OPN is decreased in PPARγ-KO MWCNT-challenged tissue at 90-days post instillation compared to 60-days. 60 and 90-day lung sections from PBS and MWCNT instilled PPARγ-KO mice were stained with antibody to OPN and counterstained with DAPI to localize nuclei. Qualitative analysis was completed on $n \geq 3$ per PBS group and $n \geq 4$ for MWCNT groups. Representative images are shown for each treatment and timepoint at 20X magnification.

Table 1. Summary of changes in MMP12 and OPN gene expression and protein in PPARγ-KO mice instilled with MWCNT at 60 and 90-days.

	MMP12	OPN
mRNA expression in BAL cells	↓	No Change
Protein in BAL fluid	No Change	↓
ICC on BAL cells	↑	↑
IHC on lung sections	↓	↓

References

1. Arkema EV, Grunewald J, Kullberg S, Eklund A, Askling J. Sarcoidosis incidence and prevalence: A nationwide register-based assessment in sweden. Eur Respir J. 2016 July 28,;48(6):1690-9.

2. Baughman RP, Field S, Costabel U, Crystal RG, Culver DA, Drent M, et al. Sarcoidosis in america. analysis based on health care use. Ann Am Thorac Soc. 2016 May 12,;12(8):1244-52.

3. Birnbaum AD, Rifkin LM. Sarcoidosis: Sex-dependent variations in presentation and management. J Ophthalmol. 2014;2014:236905.

4. Arkema E, Cozier Y. Epidemiology of sarcoidosis: Current findings and future directions. Ther Adv Chronic Dis. 2018 Aug 24,;9(11):227-40.

5. Judson M. The clinical features of sarcoidosis: A comprehensive review. Clinic Rev Alerg Immunol. 2014 Oct 2,;49:63-78.

6. Criado E, Sánchez M, Ramírez J, Arguis P, de Caralt TM, Perea RJ, et al. Pulmonary sarcoidosis: Typical and atypical manifestations at high-resolution CT with pathologic correlation. Radiographics. 2010 Oct 6,;30(6):1567-86.

7. Nunes H, Soler P, Valeyre D. Pulmonary sarcoidosis. Allergy. 2005 April 6,;5(60):565-82.

8. Judson MA. The treatment of pulmonary sarcoidosis. Respir Med. 2012 April 9,;106(10):1351-61.

9. Chen ES, Moller DR. Etiologies of sarcoidosis. Clin Rev Allergy Immunol. 2015 March 15,;49(1):6-18.

10. Du Bois RM, Goh N, McGrath D, Cullinan P. Is there a role for microorganisms in the pathogenesis of sarcoidosis? J Intern Med. 2003 Jan 10,;253(1):4-17.

11. Choo SY. The HLA system: Genetics, immunology, clinical testing, and clinical implications. Yonsei Med J. 2007 Feb 20,;48(1):11-23.

12. Judson MA. Environmental risk factors for sarcoidosis. Frontiers in immunology. 2020 June 26,;11:1340.

13. Cleven KL, Ye K, Zeig-Owens R, Hena KM, Montagna C, Shan J, et al. Genetic variants associated with FDNY WTC-related sarcoidosis. International journal of environmental research and public health. 2019 May 23,;16(10):1830.

14. Izbicki G, Chavko R, Banauch GI, Weiden MD, Berger KI, Aldrich TK, et al. World trade center "sarcoid-like" granulomatous pulmonary disease in new york city fire department rescue workers. Chest. 2007 March 30,;131(5):1414-23.

15. Wu M, Gordon RE, Herbert R, Padilla M, Moline J, Mendelson D, et al. Case report: Lung disease in world trade center responders exposed to dust and smoke: Carbon nanotubes found in the lungs of world trade center patients and dust samples. Environ Health Perspect. 2009 Dec 4,;118(4):499-504.

16. Chensue SW, Otterness IG, Higashi GI, Forsch CS, Kunkel SL. Monokine production by hypersensitivity (schistosoma mansoni egg) and foreign body (sephadex bead)-type granuloma macrophages. evidence for sequential production of IL-1 and tumor necrosis factor. J Immunol. 1989 Feb 15;142(4):1281-6.

17. Swaisgood CM, Oswald-Richter K, Moeller SD, Klemenc JM, Ruple LM, Farver CF, et al. Development of a sarcoidosis murine lung granuloma model using mycobacterium superoxide dismutase A peptide. American journal of respiratory cell and molecular biology. 2010 March 26,;44(2):166-74.

18. Werner JL, Escolero SG, Hewlett JT, Mak TN, Williams BP, Eishi Y, et al. Induction of pulmonary granuloma formation by propionibacterium acnes is regulated by MyD88 and Nox2. Am J Respir Cell Mol Biol. 2016 Sept 8,;56(1):121-30.

19. Huizar I, Malur A, Midgette YA, Kukoly C, Chen P, Ke PC, et al. Novel murine model of chronic granulomatous lung inflammation elicited by carbon nanotubes. Am J Respir Cell Mol Biol. 2011 March 18,;45(4):858-66.

20. Mohan A, Malur A, McPeek M, Barna BP, Schnapp LM, Thomassen MJ, et al. Transcriptional survey of alveolar macrophages in a murine model of chronic granulomatous inflammation reveals common themes with human sarcoidosis. American journal of physiology.Lung cellular and molecular physiology. 2018 April 1,;314(4):L617-25.

21. Hu G, Christman JW. Editorial: Alveolar macrophages in lung inflammation and resolution. Frontiers in Immunology. 2019 September 24,;10:2275.

22. Rubins JB. Alveolar macrophages. Am J Respir Crit Care Med. 2003;167(2):103-4.

23. Broos C, van Nimwegen M, Hoogsteden H, Hendriks R, Kool M, van den Blink B. Granuloma formation in pulmonary sarcoidosis. Frontiers in Immunology. 2013 Dec 10,;4:437.

24. Ricote M, Li AC, Willson TM, Kelly CJ, Glass CK. The peroxisome proliferator-activated receptor-γ is a negative regulator of macrophage activation. Nature. 1998 Jan 1,;391(6662):79-82.

25. Ricote M, Li AC, Willson TM, Kelly CJ, Glass CK. The peroxisome proliferator-activated receptor-gamma is a negative regulator of macrophage activation. Nature. 1998 Jan 1;391(6662):79-82.

26. Reddy RC. Immunomodulatory role of PPAR-γ in alveolar macrophages. J Invest Med. 2016 Jan 5,;56(2):522.

27. Huizar I, Malur A, Patel J, McPeek M, Dobbs L, Wingard C, et al. The role of PPARγ in carbon nanotube-elicited granulomatous lung inflammation. Respir Res. 2013 Jan 23;14(1):7-.

28. Culver DA, Barna BP, Raychaudhuri B, Bonfield TL, Abraham S, Malur A, et al. Peroxisome proliferator-activated receptor gamma activity is deficient in alveolar macrophages in pulmonary sarcoidosis. Am J Respir Cell Mol Biol. 2003 September 25,;30(1):1-5.

29. Fingleton B. Matrix metalloproteinases as regulators of inflammatory processes. Biochim Biophys Acta Mol Cell Res. 2017 May 11,;1864(11 Pt A):2036-42.

30. Mohan A, Neequaye N, Malur A, Soliman E, McPeek M, Leffler N, et al. Matrix metalloproteinase-12 is required for granuloma progression. Frontiers in Immunology. 2020 Sept 18,;11:2228.

31. Crouser ED, Culver DA, Knox KS, Julian MW, Shao G, Abraham S, et al. Gene expression profiling identifies MMP-12 and ADAMDEC1 as potential pathogenic mediators of pulmonary sarcoidosis. American journal of respiratory and critical care medicine. 2009;179(10):929-38.

32. Collison J. MMP12 makes the cut. Nature Reviews Rheumatology. 2018;14(9):501.

33. Lund SA, Giachelli CM, Scatena M. The role of osteopontin in inflammatory processes. Journal of Cell Communication and Signaling. 2009 Oct 2,;3(3):311-22.

34. O'Regan A. The role of osteopontin in lung disease. Cytokine Growth Factor Rev. 2003 Sept 23,;14(6):479-88.

35. Goncalves DaSilva A, Liaw L, Yong VW. Cleavage of osteopontin by matrix metalloproteinase-12 modulates experimental autoimmune encephalomyelitis disease in C57BL/6 mice. The American Journal of Pathology. 2010 Dec 16,;177(3):1448-58.

36. Maeda K, Takahashi K, Takahashi F, Tamura N, Maeda M, Kon S, et al. Distinct roles of osteopontin fragments in the development of the pulmonary involvement in sarcoidosis. Lung. 2014 Feb 14,;179(5):279-91.

37. O'REGAN A, HAYDEN J, BODY S, LIAW L, MULLIGAN N, GOETSCHKES M, et al. Abnormal pulmonary granuloma formation in osteopontin-deficient mice. Am J Respir Crit Care Med. 2001 Aug 23,;164(12):2243-7.

38. Malur A, Mohan A, Barrington RA, Leffler N, Malur A, Muller-Borer B, et al. Peroxisome proliferator-activated receptor-γ deficiency exacerbates fibrotic response to mycobacteria peptide in murine sarcoidosis model. Am J Respir Cell Mol Biol. 2019 Feb 11,;61(2):198-208.

39. Malur A, Mccoy AJ, Arce S, Barna BP, Kavuru MS, Malur AG, et al. Deletion of PPARγ in alveolar macrophages is associated with a th-1 pulmonary inflammatory response. J Immunol. 2009 May 1,;182(9):5816.

40. Celada LJ, Kropski JA, Herazo-Maya J, Luo W, Creecy A, Abad AT, et al. PD-1 up-regulation on $CD4^+$ T cells promotes pulmonary fibrosis through STAT3-mediated IL-17A and TGF-β1 production. Science Translational Medicine. 2018 Sept 26,;10(460):eaar8356.

41. Biernacka A, Dobaczewski M, Frangogiannis NG. TGF-β signaling in fibrosis. Growth Factors. 2011 Jul 11,;29(5):196-202.

42. Daniels CE, Wilkes MC, Edens M, Kottom TJ, Murphy SJ, Limper AH, et al. Imatinib mesylate inhibits the profibrogenic activity of TGF-beta and prevents bleomycin-mediated lung fibrosis. J Clin Invest. 2004 Nov;114(9):1308-16.

43. Pannu J, Nakerakanti S, Smith E, ten Dijke P, Trojanowska M. Transforming growth factor-beta receptor type I-dependent fibrogenic gene program is mediated via activation of Smad1 and ERK1/2 pathways. J Biol Chem. 2007 Apr 6;282(14):10405-13.

44. Patterson KC, Strek ME. Pulmonary fibrosis in sarcoidosis. clinical features and outcomes. Annals ATS. 2013;10(4):362-70.

45. Silva M, Nunes H, Valeyre D, Sverzellati N. Imaging of sarcoidosis. Clin Rev Allergy Immunol. 2015;49(1):45-53.

46. Spagnolo P, Sverzellati N, Wells AU, Hansell DM. Imaging aspects of the diagnosis of sarcoidosis. Eur Radiol. 2014;24(4):807-16.

47. Tashiro J, Rubio GA, Limper AH, Williams K, Elliot SJ, Ninou I, et al. Exploring animal models that resemble idiopathic pulmonary fibrosis. Frontiers in Medicine. 2017;4:118.

48. Glasser SW, Hagood JS, Wong S, Taype CA, Madala SK, Hardie WD. Mechanisms of lung fibrosis resolution. The American Journal of Pathology. 2016;186(5):1066-77.

49. Tan Q, Link PA, Meridew JA, Pham TX, Caporarello N, Ligresti G, et al. Spontaneous lung fibrosis resolution reveals novel antifibrotic regulators. Am J Respir Cell Mol Biol. 2021;64(4):453-64.

50. Zhang L, Wang Y, Wu G, Xiong W, Gu W, Wang C. Macrophages: Friend or foe in idiopathic pulmonary fibrosis? Respiratory research. 2018;19(1):170.

APPENDIX A: ANIMAL USE PROTOCOLS

ECU

Animal Care and Use Committee
003 Ed Warren Life Sciences Building | East Carolina University | Greenville NC 27354 - 4354
252-744-2436 office | 252-744-2355 fax

June 23, 2020

Mary Jane Thomassen, Ph.D.
Department of Internal Medicine, ECU

Dear Dr. Thomassen:

Your Animal Use Protocol entitled, "Carbon Nanotubes as a Tool for Generating an Experimental Model of Pulmonary Sarcoidosis" (AUP #J199d) was reviewed by this institution's Animal Care and Use Committee on 06/22/2020. The following action was taken by the Committee:

"Approved as submitted"

****Please contact Aaron Hinkle prior to any hazard use****

A copy of the protocols is enclosed for your laboratory files. Please be reminded that all animal procedures must be conducted as described in the approved Animal Use Protocol. Modifications of these procedures cannot be performed without prior approval of the ACUC. The Animal Welfare Act and Public Health Service Guidelines require the ACUC to suspend activities not in accordance with approved procedures and report such activities to the responsible University Official (Vice Chancellor for Health Sciences or Vice Chancellor for Academic Affairs) and appropriate federal Agencies. **Please ensure that all personnel associated with this protocol have access to this approved copy of the AUP/Amendment and are familiar with its contents.**

Sincerely yours,

Susan McRae, Ph.D.
Chair, Animal Care and Use Committee

SM/GD

enclosure

APPENDIX B: LIST OF Qiagen qPCR PRIMERS

Target Name	**Catalog Number**
GAPDH	PPM02946E
MMP12	PPM03619F
OPN	PPM03648C
Smad3	PPM04461C
Smad7	PPM03073F
TGFβ	PPM02991B